Chapter 4

Mass Spectrometric Sampling of a Liquid Surface by Nanoliter Droplet Generation from Bursting Bubbles and Focused Acoustic Pulses: Application to Studies of Interfacial Chemistry

(Reproduced in part with permission from Thomas, D. A.; Wang, L.; Goh, B.; Kim, E. S.; Beauchamp, J.L. *Anal. Chem.* **2015**, *87*, 3336-3344. http://dx.doi.org/10.1021/ac504494t Copyright 2015 American Chemical Society)

4.1 Abstract

The complex chemistry occurring at the interface between liquid and vapor phases contributes significantly to the dynamics and evolution of numerous chemical systems of interest, ranging from damage to the human lung surfactant layer to the aging of atmospheric aerosols. This work presents two methodologies to eject droplets from a liquid water surface and analyze them via mass spectrometry. In bursting bubble ionization (BBI), droplet ejection is achieved via the formation of a jet following bubble rupture at the surface of a liquid to yield 250 μm diameter droplets (10 nL volume). In interfacial sampling by an acoustic transducer (ISAT), droplets are produced by focusing pulsed piezoelectric transducer-generated acoustic waves at the surface of a liquid, resulting in the ejection of droplets of 100 μm in diameter (500 pL volume). In both experimental methodologies, ejected droplets are aspirated into the inlet of the mass spectrometer, resulting in the facile formation of gas-phase ions. We demonstrate the ability of this technique to readily generate spectra of surface-active analytes, and we compare the spectra to those obtained by electrospray ionization. Charge measurements indicate that the ejected

droplets are near-neutral (<0.1% of the Rayleigh limit), suggesting that gas-phase ion generation occurs in the heated transfer capillary of the instrument in a mechanism similar to thermospray or sonic spray ionization. Finally, we present the oxidation of oleic acid by ozone as an initial demonstration of the ability of ISAT-MS to monitor heterogeneous chemistry occurring at a planar water/air interface.

4.2 Introduction

Although several techniques have been utilized to achieve mass spectrometric analysis of molecular species at the liquid/vapor interface, there remains a need for further development in sampling methodology. For example, the analysis of planar liquid surfaces is not readily achieved employing FIDI-MS. This report introduces two alternative methods for mass spectrometric sampling from liquid surfaces: bursting bubble ionization (BBI) and interfacial sampling with an acoustic transducer (ISAT). As shown in Figure 4.1, both techniques achieve surface sampling by the ejection of droplets (0.5-10 nL volume) from the surface of the bulk solution. In BBI, these droplets are formed by a liquid jet following bubble bursting at the liquid/vapor interface, whereas in ISAT they are ejected by constructive interference of acoustic waves focused at the liquid surface.

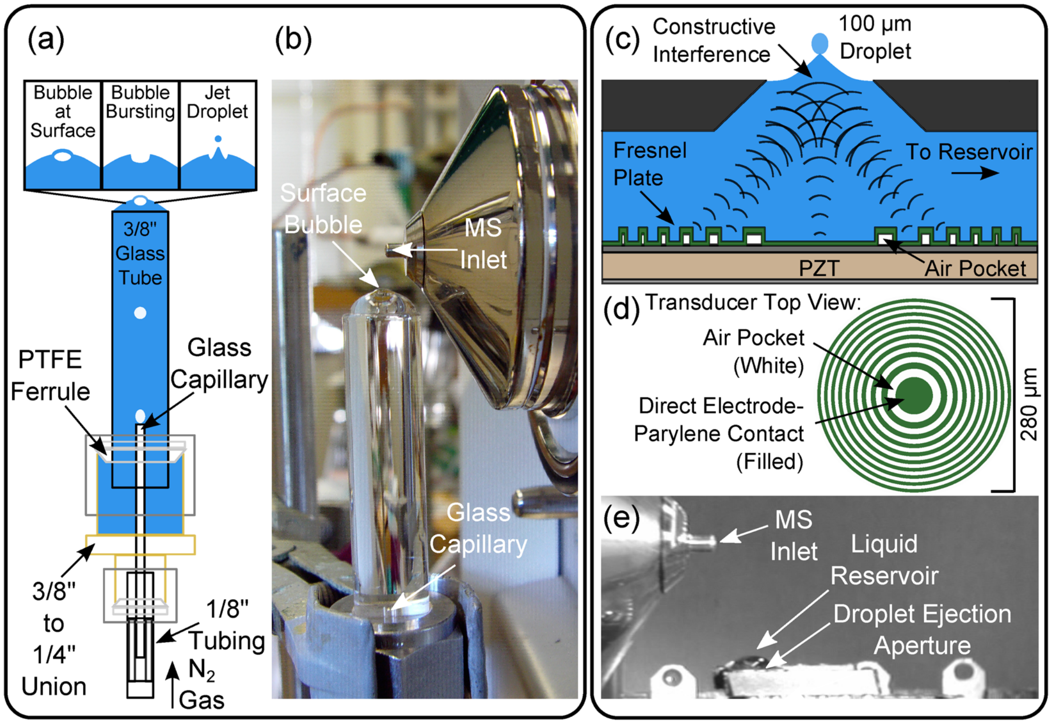

Figure 4.1. Apparatus for bursting bubble ionization (BBI) and interfacial sampling with an acoustic transducer (ISAT). The device used for BBI, which produces droplets of ~250 µm in diameter, is represented schematically in (a) and is shown interfaced with the mass spectrometer in (b). A cross section of the components of the ISAT device and an overhead view of the transducer pattern are outlined in (c) and (d), respectively. The interfacing of the device with the mass spectrometer is shown in (e).

The processes involved in bubble bursting at the water/air interface have been studied extensively for over five decades, largely in relation to their role in the generation of sea spray aerosol.[168-172] In addition, an interest in detailing the complex fluid mechanics involved in bubble bursting has led to several numerical studies.[173-176] As a bubble rises through a liquid, it may collect hydrophobic or surfactant molecules at its liquid/vapor interface, leading to enrichment of these compounds at the liquid surface.[177-182] At the liquid/vapor interface, the bubble forms a thin film layer and remains partially submerged in the liquid. As water drains from the film, the bubble becomes unstable and bursts, yielding small film droplets and leaving a cavity in the water that was previously occupied by the bubble.[183] Liquid at the surface rapidly flows in from a radial direction to fill this cavity, collecting at the center to rise up and generate a jet that ejects one or more droplets from its tip as it becomes unstable (Figure 4.1a).[172,173,175,184] Measurement of the charge on film droplets produced in pure water reveals that they typically possess a net negative charge, suggesting that formation of the film layer leads to charge separation at the liquid/vapor interface via disruption of the electrical double layer.[10] Experiments indicate that the charge on the significantly larger jet droplets is highly dependent on experimental conditions, including bubble rise time, liquid composition, ionic strength, and bubble size.[185] In addition, observations indicate that liquid in the jet droplet predominately originates in the interfacial region, suggesting that this droplet may be enriched in molecules with preference for the interface.[186,187]

Droplet ejection from a liquid surface may also be accomplished via focused acoustic pulses.[188,189] The ISAT device utilizes an acoustic transducer patterned in concentric, annular rings that generate constructive interference of acoustic waves at a single focal point on the liquid surface, similar to the diffractive focusing of light with a Fresnel zone plate (Figure 4.1c,d).[190-192] Previous experiment and theory on acoustic droplet ejection show that a liquid cone rises from the surface at the acoustic radiation focal point due to the pressure exerted on the surface, and a droplet is produced at the cone tip when this pressure surmounts the surface tension.[188,190,193] The size of the focal point, and the resulting droplet size, can be adjusted by utilizing different harmonics of the piezoelectric resonant frequency to achieve initial droplet sizes ranging from 10-100 μm in diameter, with volumes as small as 0.5 pL.[194] This device provides droplets of uniform size that are formed in a manner that incorporates surface-active molecules from the liquid reservoir.

This report details the use of both of these methods for the generation and mass spectrometric analysis of gas-phase ions from droplets ejected from a liquid surface. The presented experiments demonstrate the ability of these methods to readily detect surfactants and other molecules with nominal surface activity, compare these techniques to electrospray ionization (ESI), and suggest possible ionization mechanisms that lead to the detected gas-phase ions. It is found that these experimental methodologies are highly selective for the detection of surface-active species, which are often observed as solvent-ion adducts, consistent with a low-energy ionization process. We also utilize the ISAT device to monitor the oxidation of oleic acid by ozone as an initial demonstration of the ability of this technique to observe interfacial chemistry at a planar water/air boundary.

4.3 Experimental Methods

4.3.1 Materials

High performance liquid chromatography (HPLC)-grade methanol was purchased from J.T. Baker Avantor (Center Valley, PA), and high-purity water was purchased from EMD Millipore (Billerica, MA). All other chemicals were purchased from Sigma-Aldrich (St. Louis, MO). Stock solutions were prepared in concentrations of 5-10 mM in water or methanol using volumetric glassware. Experimental samples were then prepared by dilution of these stock solutions with use of micropipettes. Samples for BBI and ISAT were prepared in 100% water, and those for ESI were prepared in 80/20% (v/v) water/methanol due to the requirement of a lower surface tension in this experimental methodology.

4.3.2 Mass Spectrometry

All experiments were performed with use of an LTQ-XL ion trap mass spectrometer (Thermo-Fisher, Waltham, MA). ESI was performed utilizing the standard instrument electrospray source. Interfacing of ionization sources with the atmospheric pressure inlet was accomplished by removal of the spray cone for better access to the transfer capillary. Positive mode spectra were collected with a capillary temperature of 180º C, a capillary voltage of 19 V, and a tube lens voltage of 175 V. In negative mode, a capillary offset of -45 V and a tube lens voltage of -139 V were utilized.

4.3.3 Bursting Bubble Ionization (BBI)

As illustrated in Figure 4.1a, the BBI apparatus consists of a borosilicate glass tube (1/2 in. OD, 3/8 in. ID) connected via a PTFE ferrule to a 1/2 in. to 1/4 in. reducing union (Swagelok, Solon, Ohio). On the opposite side of the reducing union, a segment of 1/4 in. OD polyethylene tubing approximately 1.5 in. in length is connected. Sheathed inside of this tubing and passing through the reducing union is a glass capillary 1.6 mm in diameter with a 0.25 mm wall thickness (Kimble-Chase, Vineland, NJ). The volume of the large glass tube is filled with the sample of interest, and nitrogen gas is flowed through the inner glass capillary via a leak valve (Series 203, Brooks Granville-Phillips, Chelmsford, MA) at a flow rate optimized to form a single bubble of ~2.5 mm in diameter that rises to the liquid/vapor interface every 15 s. The apparatus is placed approximately 7-10 mm beneath the inlet to the mass spectrometer (Figure 4.1b), and bubble bursting generates a jet droplet of ~250 µm in diameter that is aspirated by the LTQ capillary inlet, resulting in the detection of ions by the mass spectrometer. The data presented in this paper consist of an average of 5 sampling events, each from a distinct jet droplet.

4.3.4 Interfacial Sampling by an Acoustic Transducer (ISAT)

The fabrication of the self-focusing acoustic transducer used for droplet generation in this work has been described previously.[190,191,193,194] The device consists of a lead zirconate titanate piezoelectric transducer (PZT) with top and bottom nickel electrodes adhesively bonded to a microfluidic device consisting of a droplet generation chamber coupled to a liquid reservoir to maintain the water height at the focal point of the acoustic waves. As shown schematically in parts c and d of Figure 4.1, a series of annular rings (Fresnel half-wave bands) consisting of air pockets under a layer of parylene D are patterned on the base of the droplet generation chamber. The air pockets reflect acoustic waves due to impedance mismatch, whereas direct contact between the parylene and the transducer electrode allows for the transmission of the acoustic waves to the liquid. Constructive interference of the transmitted acoustic waves at a focal point on the surface of the liquid results in droplet ejection. To achieve directional ejection toward the mass spectrometer inlet, a slightly modified design that introduces an unbalanced acoustic body force at the focal point was employed.[193] A radiofrequency (rf) generator was coupled to a switch to generate short rf pulses of ~10 μs in duration, which were subsequently passed through an rf amplifier and used to drive the PZT at a pulse frequency of 1-120 Hz. The device utilized was designed to operate with a focal length of 800 μm and a transducer frequency of approximately 20 MHz, the fundamental frequency, with droplet size limited by the wavelength of the acoustic waves in water (~80 μm).[188,194] The experimental amplitude and frequency of the waveform applied to the transducer were optimized to achieve droplet ejection from solution into the mass spectrometer, and the droplets generated were observed to be approximately 100 µm in diameter, corresponding to a volume of 0.5 nL. The apparatus was placed on a metal breadboard mounted to the front of the LTQ approximately 15 mm below the inlet as shown in Figure 4.1e, and droplets ejected from the surface were aspirated into the inlet of the mass spectrometer, resulting in the detection of gas-phase ions. Approximately 10-20 droplet sampling events at a rate of 1-10 Hz were averaged to generate a spectrum. For time-dependent reaction monitoring, each spectrum represents a single droplet sampling.

4.3.5 Droplet Charge Measurements

To measure droplet net charge, droplets were impacted and collected on a stainless steel plate connected to an electrometer (Model 6514, Keithley, Cleveland, OH), and the resulting current was monitored. The plate and droplet ejection apparatus were surrounded by a copper mesh to minimize interference from laboratory equipment. For the BBI experiments, the frequency of droplet ejection was too low to detect any current. A charge measurement setup was also attempted in which the charge induced on a second, electrically isolated plate was measured following droplet adhesion to the first plate, but this setup failed to yield any detectable charge on the droplets. To measure the charge on droplets generated by ISAT, the device was operated at a frequency of 60-120 Hz to provide a measurable current.

4.3.6 Ozone-Initiated Oxidation at ISAT Liquid Surface

The reaction of ozone at the surface of a planar liquid was monitored by exposing the surface of the ISAT device to a flow of the reactive gas. Ozone was generated by flowing laboratory compressed air through a glass vial containing a pencil-style ultraviolet lamp (Oriel 6035, Newport, Irvine, CA) at a rate of ~0.5 L min^{-1}. The liquid surface at the ejection aperture of the ISAT device was exposed to the gas flow via an effusive gas source. Measurement of the time-dependent oxidation of a molecule of interest was then achieved by the ejection of droplets from the ISAT device and subsequent detection as outlined above.

4.4 Results and Discussion

4.4.1 Detection of Surface-Active Species

Figure 4.2 shows the BBI and ISAT spectra for several analytes possessing high surface activity, prepared at a concentration of 50-100 μM in water. The dodecyltrimethylammonium (DDTMA, Figure 4.2b), dodecyl sulfate (DS, Figure 4.2c), and oleic acid (OA, Figure 4.2d) ions possess a hydrophobic hydrocarbon tail and hydrophilic charged headgroup that confer surfactant properties, causing these molecules to preferentially localize to the liquid/vapor interface. The peptide bradykinin (RPPGFSPFR, Figure 4.2a) possesses two terminal hydrophilic arginine residues connected by predominately hydrophobic amino acid residues that may result in surface activity for the molecule. Detection of ions in both positive mode (bradykinin, DDTMA) and negative mode (DS, OA) demonstrate that these sampling methods are capable of generating gas-phase ions of either polarity. In addition, it was observed that ions of either polarity could be detected in sampling events from the same solution, especially in BBI. For all samples, the two techniques are capable of analyte detection with good signal-to-background ratios.

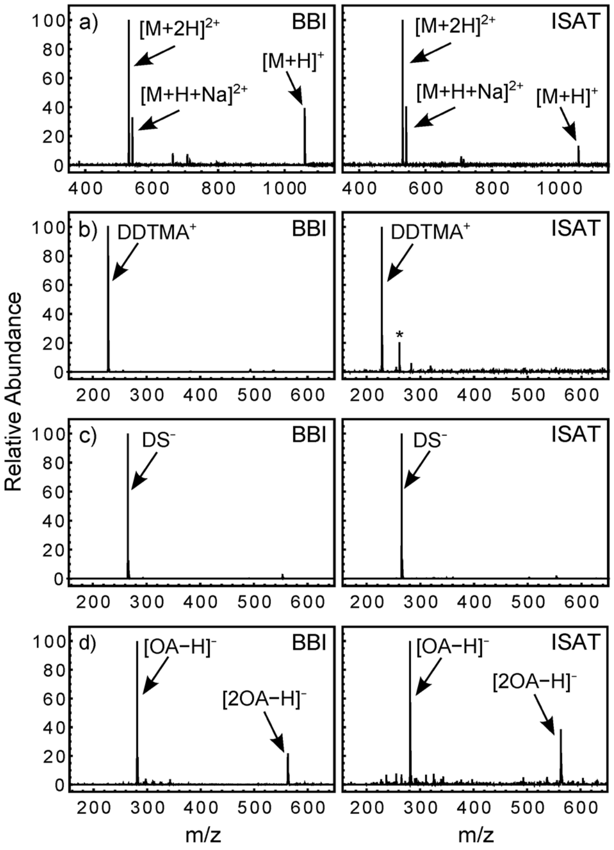

Figure 4.2. Detection of positively- and negatively-charged surface-active analytes using BBI (left column) and ISAT (right column): (a) 50 µM bradykinin, (b) 50 µM dodecyltrimethylammonium bromide (DDTMAB), (c) 100 µM sodium dodecyl sulfate (SDS), and (d) 50 µM oleic acid (OA). Asterisk in 2b indicates a contaminant present in the ISAT device (m/z 261). Surface-active species of positive (a, b) and negative (c, d) charge are readily detected in both methods, with similar spectra obtained by either technique.

4.4.2 Preferential Ionization of Surface-Active Species

The preferential ionization of surface-active compounds is a well-known phenomenon occurring in ESI.[111] To gain insight into the gas-phase ion generation process of the droplet ejection-based methodologies, the preferential ionization of surface-active analytes in BBI and ISAT spectra was analyzed and compared to results from ESI. Figure 4.3 shows the spectrum obtained by sampling an equimolar solution of sodium iodide and sodium bromide employing ESI, BBI, and ISAT. The BBI and ISAT methods tend to produce significantly more water adducts of bromide and iodide than ESI, with BBI yielding the largest abundance of these species. Given the low free energies associated with halide water adduct formation in the gas phase (~22 and ~30 kJ/mol for bromide and iodide, respectively),[195-197] it is possible that these adducts arise following gas-phase ion formation, as has been observed previously via the addition of solvent vapors to the sheath gas of an ESI source.[198] The comparatively large volume of droplets in BBI and ISAT will increase the vapor pressure of water within the capillary and vacuum transfer region of the mass spectrometer, resulting in increased adduct production. Alternately, the adduct formation may occur during the process of droplet evaporation and gas-phase ion generation.

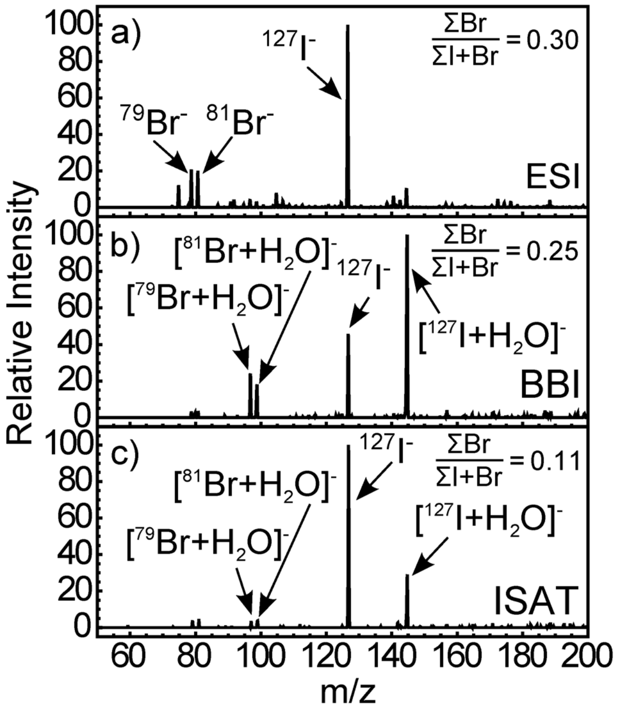

Figure 4.3. Preferential ionization of iodide over bromide in an equimolar solution (10^{-4} M) of the sodium salts. BBI and ISAT (b and c) yield a stronger response for iodide than bromide when compared with ESI (a), with ISAT yielding the largest difference in response between the two species. BBI and ISAT also tend to yield significantly more water adducts than ESI.

Also of note in the spectra of Figure 4.3 is a higher abundance of I^- over Br^-. This effect has been observed previously in ESI and is attributed to selective enrichment of iodide ions during the charged droplet discharge process, in which charged molecules preferentially localized to the liquid/vapor interface (i.e., those ions with less favorable solvation energies) are conducted along the surface of the droplet and serve as charge carriers in the progeny droplets.[199] Alternately, the difference in abundance in ESI may be explained by the ion evaporation model, in which the lower solvation energy of the iodide ion compared with that of the bromide ion results in preferential evaporation of iodide and thus a higher abundance of gas-phase ions of this species.[200] The preference of large, polarizable halide ions for the liquid/vapor interface has also been noted in molecular dynamics simulations of alkali metal halide solutions.[11,15,32,34] The BBI and, to a more pronounced extent, ISAT spectra exhibit greater selectivity for iodide over bromide than ESI, which may be a result of either enrichment of molecules present at the liquid/vapor interface during droplet generation or differences in the ionization process that lead to altered preferential ionization of surface-active species. Similar results were observed for the preferential ionization of surface-active tetraethylammonium ions over the well-solvated cesium ions in an equimolar solution.

4.4.3 Charge Measurement of Ejected Droplets

The mechanism of gas-phase ion production in electrospray ionization requires the generation of charged droplets that undergo subsequent evaporation and Rayleigh discharge to yield progeny droplets carrying <5% of the volume and 20-30% of the charge of the parent droplet.[111,201-203] Transfer of ions to the gas phase is also observed in techniques where droplets are formed without the application of an electric field, such as sonic spray ionization (SSI), in which charged droplet formation is proposed to occur via statistical fluctuations of ion concentration during droplet formation and/or the segregation of charges during droplet breakup within the atmospheric pressure interface of the mass spectrometer.[72,112,204,205] To investigate the possible mechanisms involved in ion formation in BBI and ISAT, measurement of the charge on the ejected droplets was undertaken.

Droplets were ejected from a liquid surface using the ISAT device at a rate of 60 or 120 Hz and collected on a stainless steel plate connected to an electrometer to measure the generated current. As summarized in Table 4.1, these experiments indicate that ejected droplets possess a small but measurable charge. The HPLC grade water may still contain a significant number of charge carriers other than the hydronium and hydroxide ions, as the liquid was not further purified, and plasticizers and other unidentified compounds could be detected in the mass spectrum by ISAT of pure water samples. The charge of surface-active molecules in the sample influences the net charge of the droplets generated, with the polarity of the measured current dictated by the charge of the analyte. For all samples examined in these experiments, less than 5×10^4 net charges per droplet were estimated, putting these droplets significantly below the Rayleigh limit for droplet discharge (<0.1%) at the initial droplet diameter.[111,206] To reach the Rayleigh limit by evaporation, a water droplet containing this number of charges would have to evaporate to approximately 1 µm in diameter. For comparison, if a stream of droplets of 100 µm in diameter were produced by ESI, they would be initially charged to approximately 80% of the Rayleigh limit, produce a current of 700 pA at an impact rate of 120 Hz, and undergo Rayleigh discharge at a droplet diameter of 88 µm.[201] As discussed below, the time scale of droplet transfer to the high vacuum region of the mass spectrometer is not sufficient for the droplets generated by ISAT to reach the Rayleigh limit via evaporation, suggesting alternate ionization mechanisms are operative under the experimental conditions.

Table 4.1. Measured Current for Droplets 100 μm in Diameter Produced by the ISAT device and Collected on a Stainless Steel Plate at Given Rate[a]

sample	droplet pulse rate (Hz)	measured current (pA)	charges/ droplet	% Rayleigh limit
HPLC grade water	60	0.1	1×10^4	0.02
100 μM CsI, 100 μM TEAB in water	120	0.5	3×10^4	0.06
50 μM SDS in water	120	−0.2	1×10^4	0.02

[a]Net charge per droplet and percentage of the Rayleigh limit are calculated.

4.4.4 Droplet Residence Time and Evaporation

The proposed mechanism for ion formation must be consistent with the temporal constraints imposed by the droplet sampling from the vapor phase through the inlet capillary of the mass spectrometer. The transfer time of a droplet through the mass spectrometer inlet capillary is dependent upon the gas flow rate through the inlet, which can be approximated using the Poiseuille equation,[205,207]

$$Q = \frac{\pi r^4}{8\eta L}\Delta P \tag{4.1}$$

where ΔP represents the pressure difference across the inlet (759 Torr), r is the radius of the transfer capillary (250 μm), η is the dynamic viscosity of air (2.5×10^{-5} Pa s at 450 K),[208] L is the capillary length (100 mm), and Q is the volumetric flow rate. This equation yields a volumetric gas flow of 4.2×10^{-5} m^3 s^{-1}, or a gas velocity of ~200 m/s and a gas transfer time of ~0.5 ms, which agrees reasonably well with the gas flow at the MS inlet of ~1×10^{-5} m^3 s^{-1} determined with use of a Gilibrator (Sensidyne, St. Petersburg, FL). Although this approximation does not take into account the change in gas flow velocity across the transfer tube, the transfer time was also found to be in good agreement with previous studies and serves as an order of magnitude estimate for gas transfer time.[205,209,210]

When the aspirated droplet initially enters the capillary, its velocity along the axis of the capillary is near zero, and the acceleration of the droplet to the carrier gas velocity requires a non-negligible amount of time. This rate of acceleration can be estimated from the drag force F_D exerted on the droplet by the flowing gas, given by[211]

$$F_D = C_D \frac{\pi}{8} \rho_g d^2 \left(v_{gas} - v_{droplet}\right)^2 \tag{4.2}$$

where C_D is the coefficient of drag (~0.44 at the high Reynolds numbers encountered in this system),[211] ρ_g is the gas density (~1 kg/m^3),[208] d is the droplet diameter, v_{gas} is the gas velocity, and $v_{droplet}$ is the droplet velocity. Neglecting the effects of turbulent flow, the timescale for droplet transit across the capillary can be estimated by accounting for the acceleration caused by the drag force on the droplet to yield the differential equation

$$m \frac{d^2x}{dt^2} = C_D \frac{\pi}{8} \rho_g d^2 \left(v_{gas} - \frac{dx}{dt}\right)^2 \tag{4.3}$$

For a droplet of diameter 100 µm, the calculated transit time across a 100 mm capillary is approximately 15 ms.

The rate of change of a droplet of diameter d due to evaporation is given by[211]

$$\frac{d(d)}{dt} = \frac{4D_v M}{R\rho_d d}\left(\frac{p_\infty}{T_\infty} - \frac{p_d}{T_d}\right) \tag{4.4}$$

where M is the solvent molar mass, D_v is the diffusivity of the solvent vapor in air, ρ_d is the solvent density, and R is the gas constant. The solvent partial pressure well away from the droplet surface and at the droplet surface are represented by p_∞ and p_d, respectively, and the corresponding temperatures are denoted by T_∞ and T_d. Integrating this equation yields the droplet evaporation rate as a function of time[211,212]

$$d^2 = d_0^2 + \frac{8D_vM}{R\rho_d}\left(\frac{p_d}{T_d} - \frac{p_\infty}{T_\infty}\right)t \tag{4.5}$$

where d_0^2 is the initial droplet diameter. The solvent evaporation process is endothermic, lowering the temperature at the droplet surface, T_d, until equilibrium between evaporative cooling and heat conduction from the surrounding air is achieved. This steady state temperature can be calculated by[211]

$$T_d = T_\infty - \frac{D_vM\Delta H_{vap}}{Rk_v}\left(\frac{p_d}{T_d} - \frac{p_\infty}{T_\infty}\right) \tag{4.6}$$

where ΔH_{vap} is the solvent enthalpy of vaporization at temperature T_d and k_v is the thermal conductivity of the gas. Since many of the parameters in equation 4.6 are temperature-dependent, specifically D_v, p_d,, ΔH_{vap}, and k_v, the equation must be solved for T_d iteratively until a self-consistent temperature is achieved. The solvent enthalpy of vaporization and equilibrium vapor pressure were taken from Yaws,[213] the diffusion coefficient of water in air was taken from Vargaftik *et al.*,[214] and the thermal conductivity of air was taken from Kadoya *et al.*[215] The value of p_∞ was approximated by the partial pressure of water vapor in air at 50% relative humidity at 298 K,[213] and T_∞ was set to the transfer capillary temperature (450 K). These parameters give an equilibrium droplet surface temperature, T_d, of 318 K, which was used for the calculation of the droplet diameter as a function of time according to equation 4.5, with solvent density at this temperature taken from *The CRC Handbook of Chemistry and Physics*.[208]

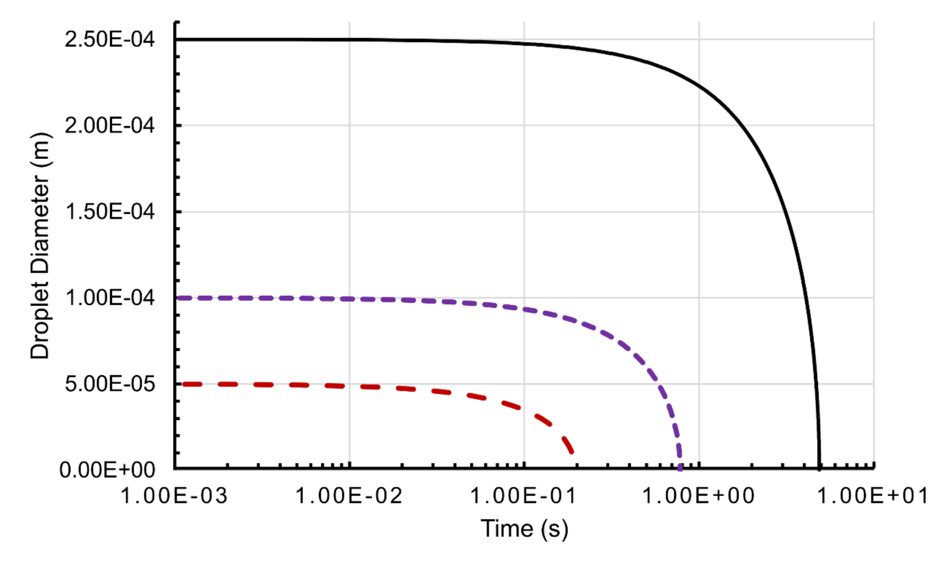

Figure 4.4. Calculated change in droplet diameter with time for droplets of diameter 50 µm (red, large dash), 100 µm (purple, small dash), and 250 µm (black, solid line) at a gas temperature of 450 K and a water vapor pressure of 1571 Pa (50% relative humidity at 298 K). The time axis is presented on a logarithmic scale. See text for details.

The graph of droplet diameter as a function of time calculated from equations 4.5 and 4.6 is shown in Figure 4.4 for droplets of diameter 50, 100, and 250 µm, which are found to evaporate in 200 ms, 780 ms, and 4.9 s, respectively. Thus, for the 100 and 250 µm diameter droplets utilized in this study, the evaporation time is longer than the calculated 15 ms residence time by several orders of magnitude.[201,205,212] In addition, the high Weber number conditions present within the transfer capillary suggest the droplet will undergo aerodynamic breakup into smaller droplets during transit.[205,216,217] Therefore, it is not likely that droplet evaporation to the Rayleigh limit followed by droplet discharge could produce the observed ions, and other ionization mechanisms must be explored.

4.4.5 Ionization Mechanism in BBI and ISAT

Given the relatively large diameter (100-250 µm) of droplets utilized in this study in comparison to the inner diameter of the transfer capillary (~1 mm), droplet nebulization via interaction with the heated walls of the capillary may contribute significantly to the ionization process. A similar phenomenon has been observed previously by Vestal and co-workers in thermospray ionization. In this technique, the eluent from a liquid chromatography column is flowed into a heated capillary, resulting in the nebulization and partial vaporization of the solvent.[218,219] This process generates charged droplets, most likely as a result of statistical fluctuations in ion concentration,[204] that subsequently follow the ESI mechanism.[220,221] A similar process may also occur in the solvent-assisted inlet ionization technique developed by Trimpin, McEwen, and co-workers.[222,223] In addition, Jarrold and co-workers found that highly charged droplets may be generated from larger, near-neutral droplets in sonic spray ionization via charge separation during the aerodynamic breakup of droplets.[205] Such processes may also be operative in other droplet generation techniques that do not rely on electric fields, including easy ambient sonic spray ionization (EASI) and ultrasonication-assisted spray ionization (UASI).[224-226] These putative mechanisms are compatible with the data presented in this work and account for the tendency of BBI and ISAT to yield water adducts (Figure 4.3) as well as the ability to observe positive and negative ions with identical sampling conditions.

4.4.6 Monitoring Heterogeneous Chemistry with ISAT

As an initial demonstration of the ability of the ISAT droplet ejection technique to monitor heterogeneous chemistry, we studied the time-dependent oxidation of oleic acid by ozone. This system is regarded as a benchmark to compare experimental methodologies for the study of interfacial oxidation.[27,83,227-230] As summarized in Scheme 4.1, oxidation of oleic acid proceeds via formation of a primary ozonide, followed by ring opening to the right or left to yield nonanal (**1**) or 9-oxononanoic acid (**2**), respectively, along with the corresponding Criegee intermediate. These intermediates may then proceed along numerous reaction pathways, including formation of secondary ozonides, peroxides, diperoxides, and α-acyloxyalkyl hydroperoxides, which may subsequently undergo decomposition or polymerization to yield a complex set of products.[227,228] Although measured yields are highly sensitive to experimental conditions, the most abundant products generally observed in oleic acid oxidation are nonanal (**1**) and 9-oxononanoic acid (**2**), with slightly lower abundances of nonanoic acid (**3**) and azelaic acid (**4**).[229,230] A previous study by Grimm and co-workers utilizing FIDI-MS to study the oxidation of oleic acid dissolved in 90/10 (v/v) dimethylformamide/methanol observed azelaic acid as the most abundant product detectable as an anion, suggesting that the solvent plays a crucial role in determining the favored reaction pathway.[83]

Scheme 4.1. Oxidation of Oleic Acid by Ozone and Subsequent Reaction Pathways

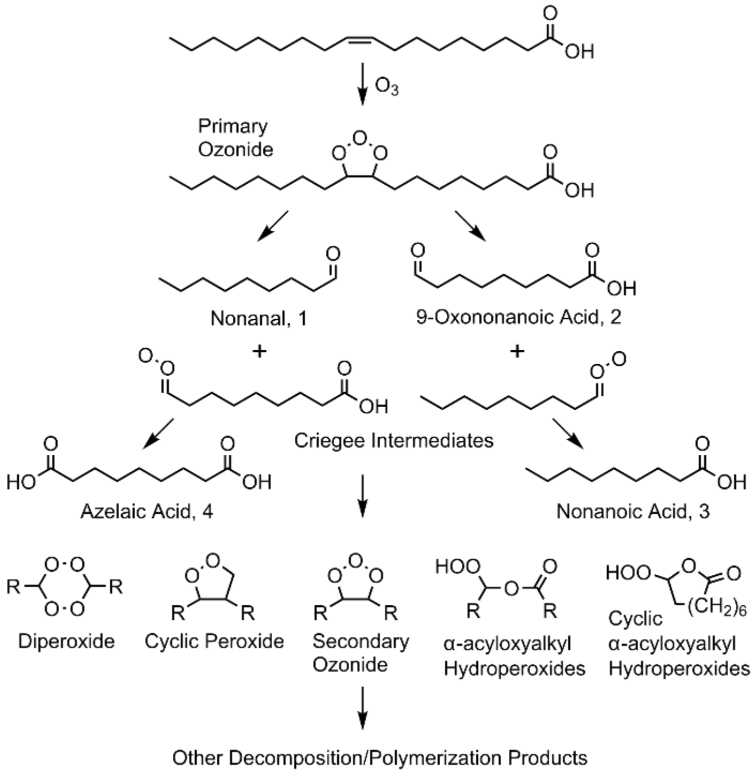

For study of the oxidation of oleic acid using the ISAT methodology, a solution containing oleic acid at a concentration of 100 µM and a small amount of sodium dodecyl sulfate (< 10 µM) as a nonreactive, surface-active reference species in water was loaded into the device. The liquid surface at the droplet ejection aperture was then exposed to a flow of air containing ozone generated by ultraviolet photodissociation of oxygen. Droplets were sampled from the surface at several time points during the experiment to monitor the progress of the reaction. As shown in Figure 4.5, the oleic acid anion is observed to decay in intensity over the course of the experiment, whereas the nonreactive dodecyl sulfate (DS) anion is detected even at long exposure times. The main product detected from oleic acid oxidation is 9-oxononanoic acid (9-ONA), in agreement with the majority of previous studies of oleic acid oxidation.[230] Nonanal is also frequently reported as a major product of oleic acid oxidation but could not be detected by the mass spectrometer in negative mode due to the absence of a negatively charged functional group. Although the droplet formation process disturbs the structure of the interface in a manner that may influence what is subsequently observed in the mass spectrum relative to what originally comprised the surface, sequential sampling was still capable of observing the progression of oleic acid oxidation in this experiment.

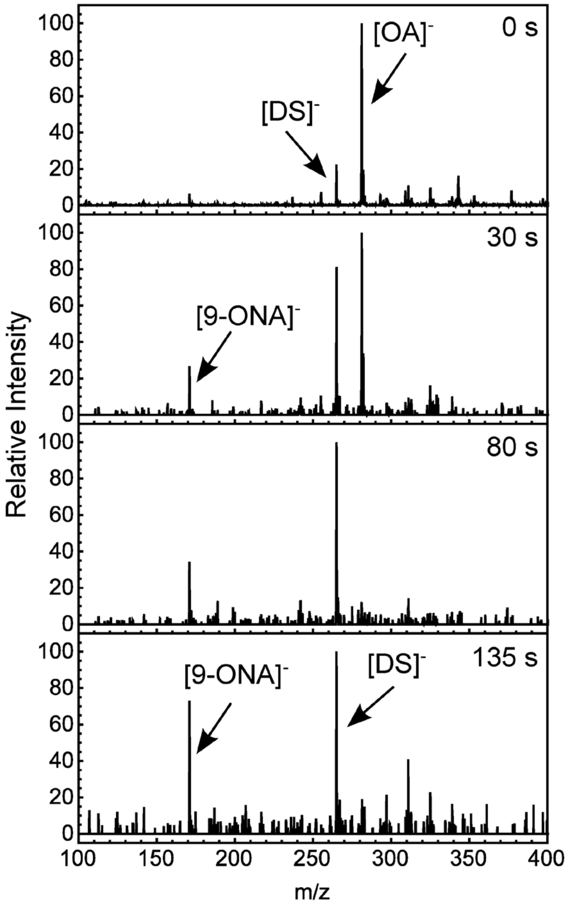

Figure 4.5. Time-dependent oxidation of oleic acid (OA) at a liquid surface by impinging gas-phase ozone, as monitored by ISAT-MS. A small amount of dodecyl sulfate (DS) serves as a nonreactive reference species at the interface. During the experiment, the oleic acid disappears from the spectra and is replaced by 9-oxononanoic acid (9-ONA).

4.5 Conclusions

Two new methods for the ejection of droplets from nominally planar surfaces are coupled with mass spectrometry to study the chemistry of liquid surfaces. Droplets are produced either by bubble bursting and subsequent jet formation or through the acoustic radiation pressure exerted on a liquid surface by focused acoustic waves. The droplets generated by these methodologies can be aspirated by the heated transfer capillary of a mass spectrometer, yielding gas-phase ions of both positive and negative polarity from surface-active analytes with high sensitivity. The ability to generate ions from near-neutral droplets on a time scale much shorter than that required for droplet evaporation to the Rayleigh limit suggests that droplet breakup, nebulization, and vaporization may occur within the heated transfer capillary to assist in the production of gas-phase ions.

The use of droplet ejection to study chemical reactions at liquid surfaces via mass spectrometry has many promising future applications. The ability to monitor the reactions of complex chemical systems occurring at liquid surfaces is highly complementary to the detailed structural information provided by surface-sensitive spectroscopic techniques.[42,231] The ISAT device in particular allows for the controlled generation of droplets from a planar liquid surface on demand, making this methodology readily amenable to the study of heterogeneous chemical reactions, such as the reaction of gas-phase hydroxyl radicals and ozone with surface-active analytes in solution.[7,48,83,229,232,233] We provide in this work results for the oxidation of oleic acid by ozone as an initial example of the ability of the ISAT device to monitor heterogeneous reactions at the liquid/vapor interface. The ISAT methodology may prove especially useful for the study of planar liquid surfaces. For example, the ISAT apparatus may be integrated with a Langmuir-Blodgett trough to study the effect of surface pressure on the structure and reactivity of surface films, especially with respect to the spatial separation of analytes at increased pressures.[234-236] In addition, operation of an ISAT apparatus designed to function at higher harmonics can produce droplets as small as 10 µm in diameter (500 fL volume),[194] and optimization of this configuration for mass spectrometric sampling may lead to decreased disruption of the interfacial layer and will likely enhance specificity for sampling of species present at the liquid/vapor interface.